

## Supplemental Data

### LEGENDS TO SUPPLEMENTAL FIGURES

**Figure S1.** Increased pH sensitivity of  $K^+$  conductance in cells expressing heteromeric Kir4.1/Kir5.1 channels. Representative currents measured on cell, and on excised membrane patches exposed to pH 8.5, 7.5, 6.5 and 5.5, in cells transfected with WT Kir4.1 (**A**) or co-transfected with WT Kir4.1 and Kir5.1, at a 1:1 ratio (**B**). The pulse protocol is shown in the upper left. Pipette and external solution were  $K_{INT}$  buffer at pH 7.5. Dotted line indicates zero current.

**Figure S2.** Disruption of the inter-subunit E288–R297 salt bridge accounts for the effect of R297C. **A–B**, Time-course of relative  $^{86}Rb^+$  efflux in mock-transfected control cells and in cells expressing WT, E288C, R297C or the double mutant E288C-R297C, in homomeric Kir4.1 (**A**) and in heteromeric Kir4.1/Kir5.1 channels (**B**). **C**, Rate constants for Kir4.1-dependent (white bars) and Kir4.1/Kir5.1-dependent (gray bars)  $^{86}Rb^+$  efflux  $k_2$ , as obtained by fitting flux data to equation (1). Results are means  $\pm$  s.e.m. of 3–12 experiments, each in triplicate. Data for control, WT and R297C are the same as in Fig. 2 and Fig. 3.

**Figure S3.** The intra-subunit C108–C140 disulfide bond is essential for channel function, and cannot be replaced by a salt bridge. **A–B**, Time-course of relative  $^{86}Rb^+$  efflux in control cells and in cells expressing WT, C108E, C140R or the double mutant C108E-C140R, in homomeric Kir4.1 (**A**) and in heteromeric Kir4.1/Kir5.1 channels (**B**). **C**, Rate constants for Kir4.1-dependent (white bars) and Kir4.1/Kir5.1-dependent (gray bars)  $^{86}Rb^+$  efflux  $k_2$ , as obtained by fitting flux data to equation (1). Results are means  $\pm$  s.e.m. of 3–12 experiments, each in triplicate. Data for control, WT and C140R are the same as in Fig. 2 and Fig. 3.

Figure S1.

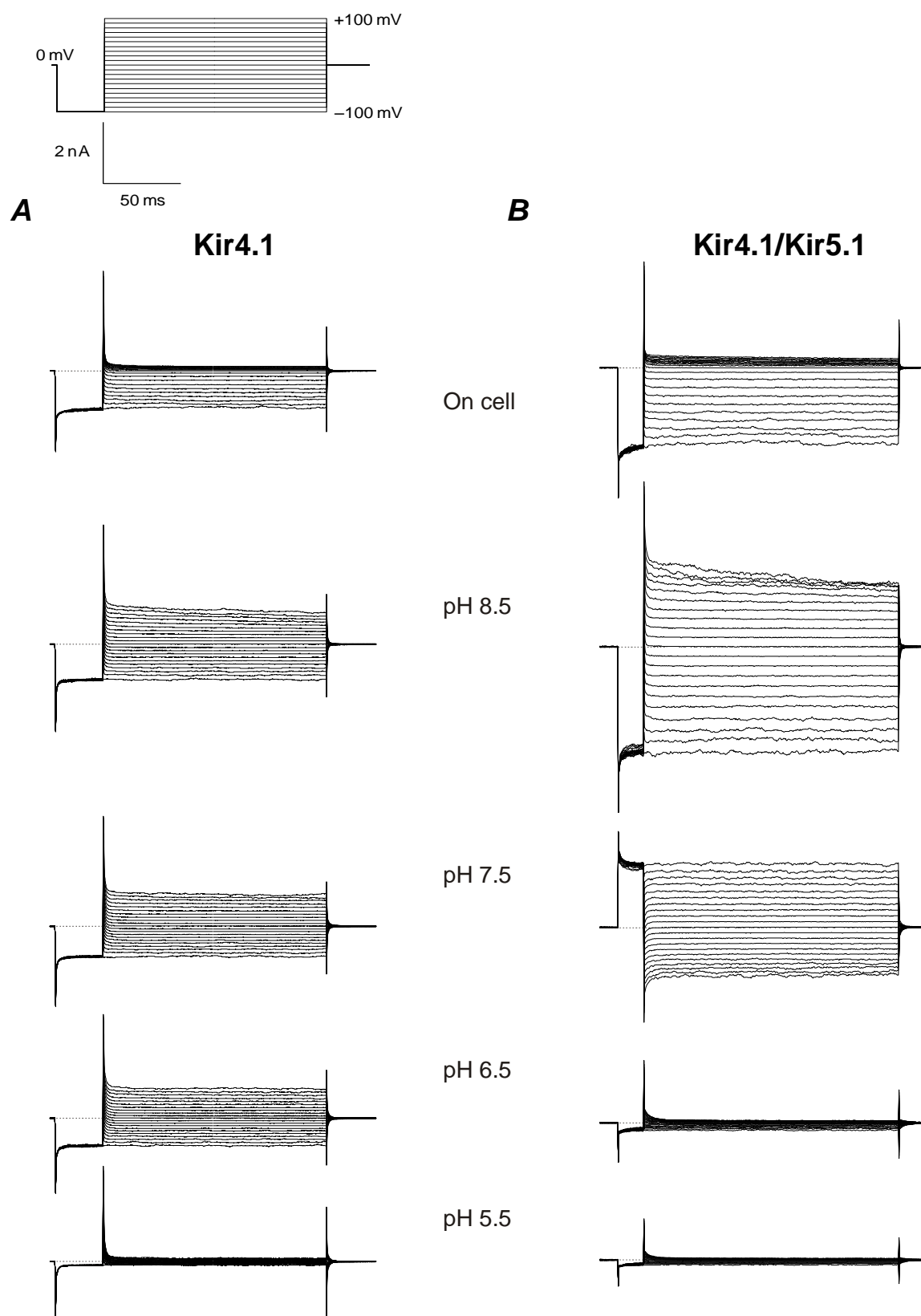


Figure S2.

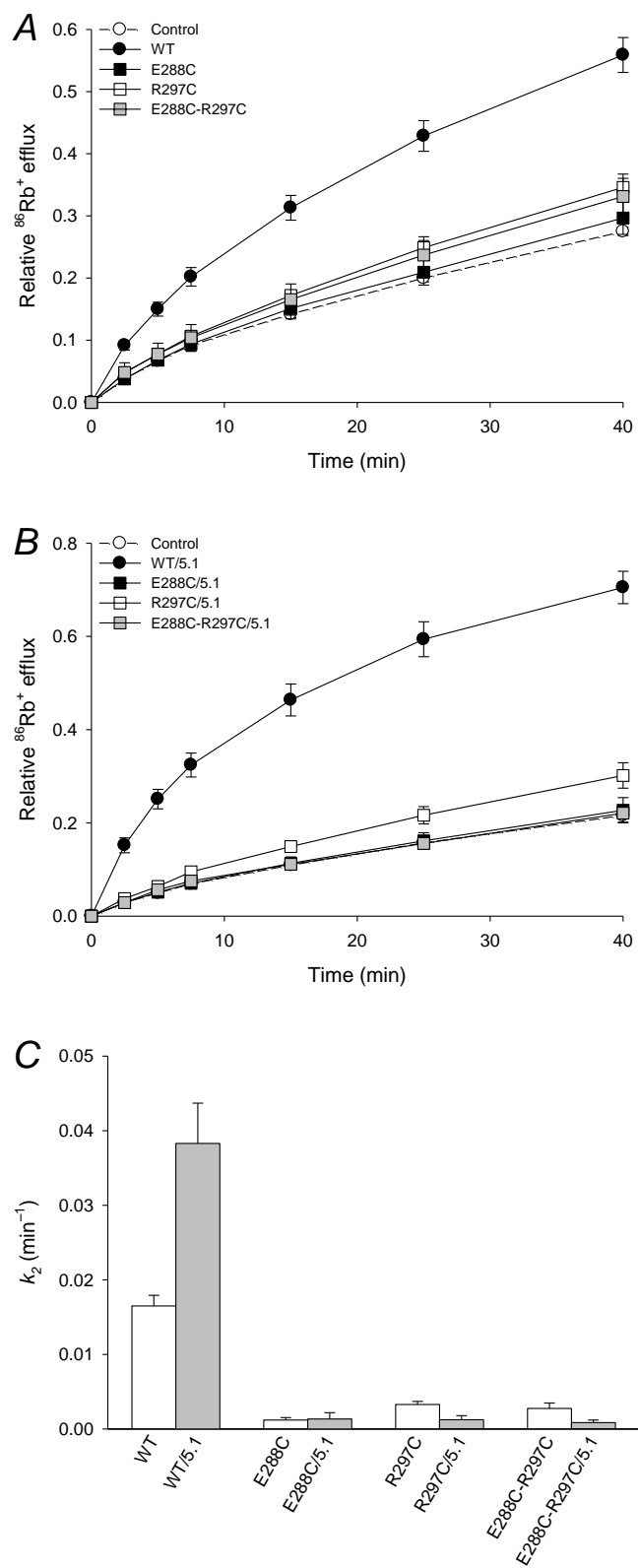


Figure S3.

